Supporting Information

Insights into conversion mechanism of restriction strategy and self-activation enabled high-performance manganese fluoride anodes

Jun Wu,[a1] Jiamao Hao,[c1] Chengdeng Wang,[a] Haofeng Shi,[a] Fang Zhu,[a] Lu Yang,[a] Zhiming Bai,[b] Xiaoqin Yan,[a*] and Yousong Gu[a*]*

[1] These authors contributed to the work equally and should be regarded as co-first authors.

[a] School of Materials Science and Engineering, University of Science and Technology Beijing, Beijing 100083, PR China

[b] School of Civil and Resource Engineering, University of Science and Technology Beijing, Beijing, 100083, PR China

[c] Defense Innovation Institute, Academy of Military Science, Beijing 100071, PR China

*Corresponding author
E-mail: yousongu@mater.ustb.edu.cn; xqyan@mater.ustb.edu.cn; baizhiming@ustb.edu.cn

Experimental Section

Precursors Preparation: The precursor NH_4MnF_3 was synthesized by microemulsion (ME) method with NH_4F and $MnCl_2$ as raw materials. Cyclohexane (70 mL), Cetyltrimethylammonium bromide (CTAB, 10 g), and NH_4F aqueous solution (0.03 mol L^{-1}, 15 mL) were mixed with magnetic stirring, and n-Butanol was added dropwise until a transparent and stable microemulsion was formed. After fully stirring for 30 min, $MnCl_2$ aqueous solution (0.01 mol L^{-1}, 15 mL) was slowly poured and the microemulsion still maintained a stable state. After 1 h of reaction, ethanol was added for demulsification and centrifugation, repeated washing with ethanol and centrifugation for 3 times, and dried to obtain the precursor. For comparison, the raw materials with the same concentration were added to the aqueous solution to synthesize the precursors.

MFMC Preparation: The pH of the trometamol aqueous solution (0.01 mol L^{-1}) was adjusted to 7.0 with diluted hydrochloric acid (0.12 mol L^{-1}). After ultrasonic dispersion of NH_4MnF_3 powder in tris buffer, tannic acid (1.5 times the mass of NH_4MnF_3) was added for coating, and stirring for more than 12 h to ensure that tannic acid was fully self-polymerized on the powder surface. The mixture was centrifuged, washed, and dried to obtain a tannic acid-coated precursor. The heat treatment process of composite precursor calcination was determined by TGA. The sample was heated from room temperature to 650 ℃ (5 ℃ min^{-1}) under nitrogen atmosphere and maintained for 2 h, and target product was obtained after cooling.

Materials Characterization: X-ray diffraction patterns (XRD, Ultima IV SmartLab) were used to reveal phase composition and crystal structure of the precursor and calcined product. Raman spectrometer (Horiba Evaluation, 532 nm laser) and Fourier-transform infrared spectroscopy (FT-IR, Thermo Scientific Nicolet iS20, 400-4000 cm^{-1}) were used to analyze the composition and structure of the coating layer. X-ray photoelectron spectroscopy (XPS) was used to determine the information of elemental and chemical state of materials. Brunauer-Emmett-Teller (BET) surface area, Field-emission scanning electron microscope (FE-SEM, Gemini-500), Transmission electron

microscope (TEM, JEOL JEM-2100F, operating voltage 200 keV) were used to observe the structure and morphology of materials.

Electrochemical Measurements: MnF_2 usually serves as the anode for rechargeable Li batteries, and its electrochemical performance was explored in coin cells (CR2025) with Li foil as the counter electrode. The electrode material was composed of active material, conductive carbon black (super P) and polyvinylidene difluoride (PVDF) (mass ratio 8:1:1), which was dissolved in N-Methylpyrrolidone (NMP) and mixed uniformly, then coated on copper foil, The average active material loaded on each electrode was 0.56 mg. The electrolyte composition was 1 M $LiPF_6$ dissolved in EC and DMC (volume ratio 1:1) with 5% FEC, and each coin cell contained 20 μL of the electrolyte. The Celgard 2500 film was used as a diaphragm, and the cells were assembled in an argon filled glove box. The long cycles and rate performances of battery were tested by NEWARE within the voltage window of 0.01-0.3 V. The charge-discharge range for galvanostatic intermittent titration technique (GITT) is 0.01-3V, with a constant current duration of 10 minutes and a relaxation time of 30 minutes in each period. Cyclic voltammetry (CV) with the voltage range of 0.01-3 V and electrochemical impedance spectroscopies (EIS) with the frequency range of 0.1-100000 Hz were tested on the CHI660e electrochemical workstation.

DFT Calculations: All the calculations were performed using the Vienna Ab initio Simulation Package (VASP) with Density Functional Theory (DFT) and Projector Augmented Wave (PAW) method, and the kinetic energy cutoff was set to 500 eV. The diffusion barrier of Li^+ was obtained by Climbing Image-Nudged Elastic Band (CI-NEB). The first Brillouin zone was sampled by a 5×5×1 k-point grid within the Monkhorst-Pack scheme. The exchange-correlation interactions were treated by Generalized Gradient Approximation (GGA) and Perdew-Burke-Ernzerhof functional (PBE). The geometric relaxation ended when the total force per atom was less than 0.01 eV $Å^{-1}$ and the electron self-consistent cycle converged to 10^{-6} eV.

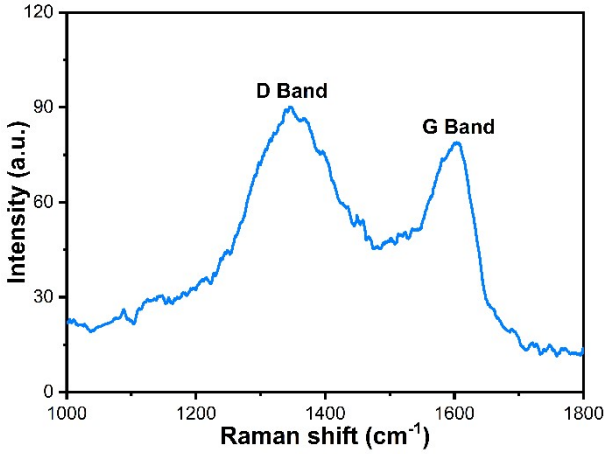

Figure S1 Raman spectrum of MFMC.

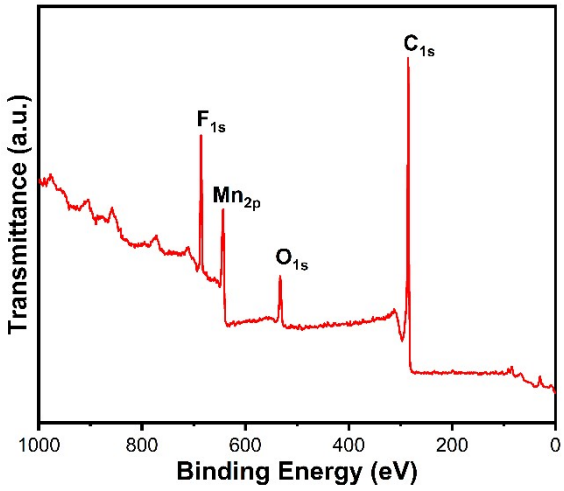

Figure S2 XPS survey of MFMC.

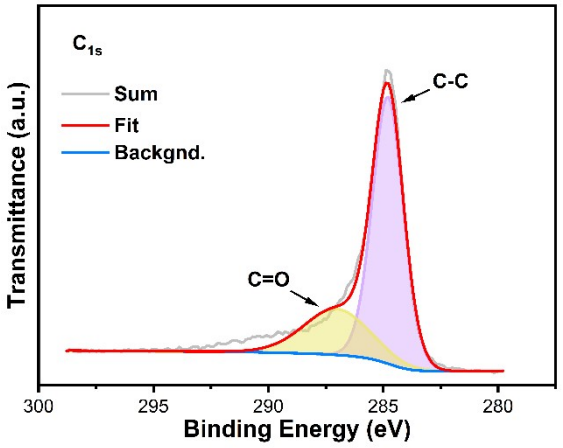

Figure S3 XPS spectrum of C1s.

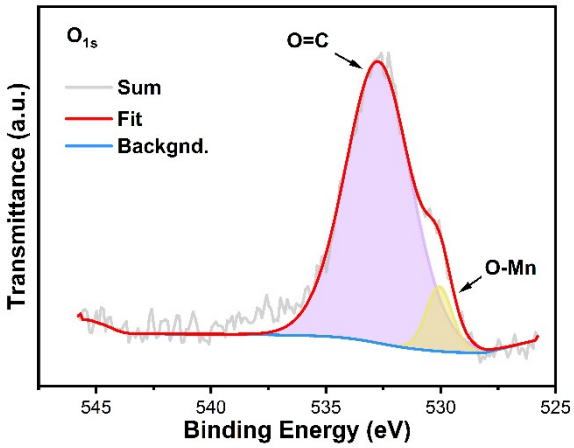

Figure S4 XPS spectrum of O1s.

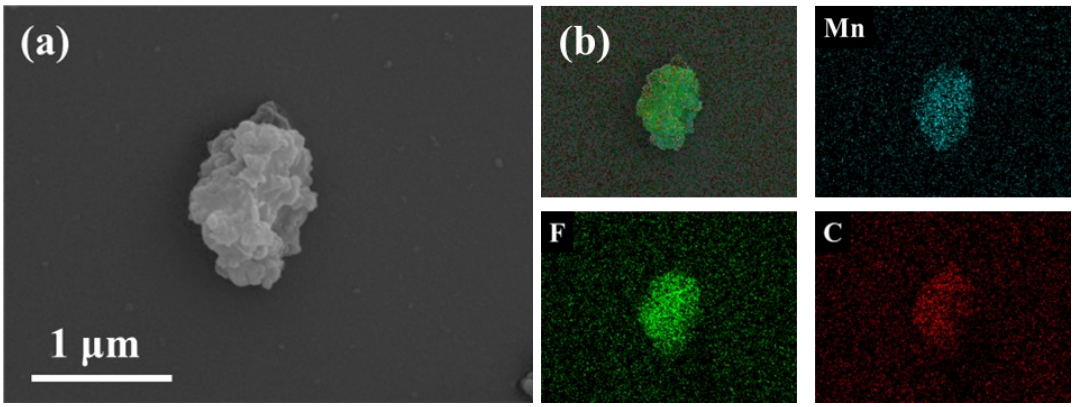

Figure S5 a) SEM image and b) EDS of MFMC.

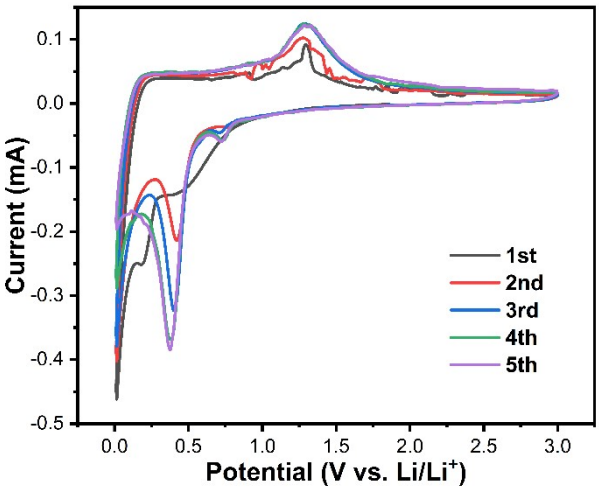

Figure S6 CV curves of MnF_2.

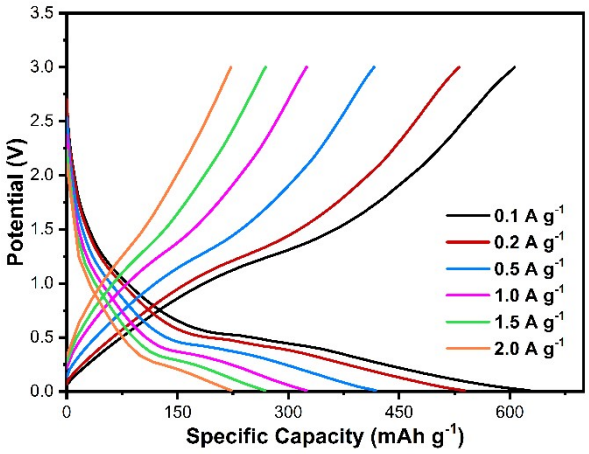

Figure S7 Discharge/charge capacity-voltage curves of MFMC at different current rates.

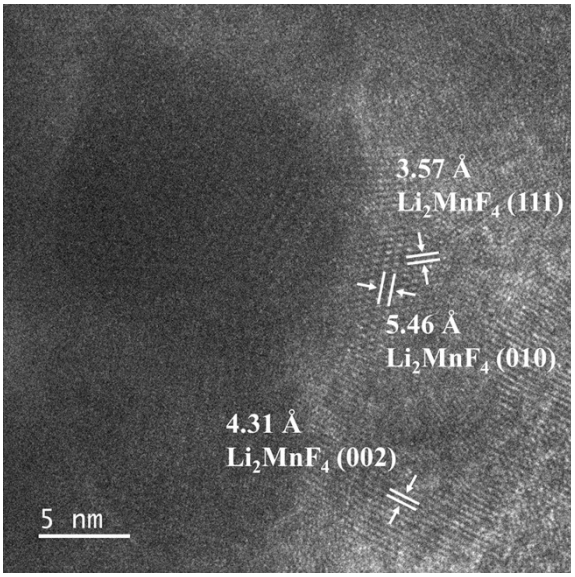

Figure S8 Lattice stripes of Li_2MnF_4.

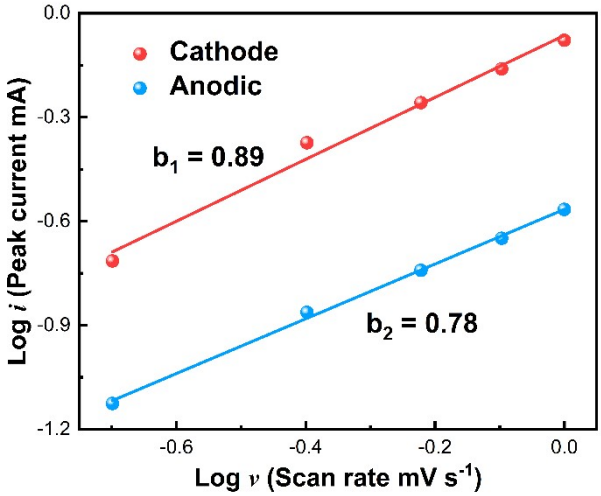

Figure S9 The b-values determined from the evolution of peak currents with different sweep rates.

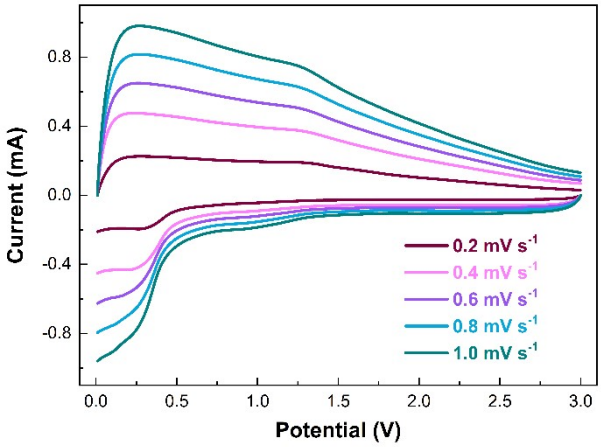

Figure S10 Calibrated CV curves of MFMC at various scan rates.

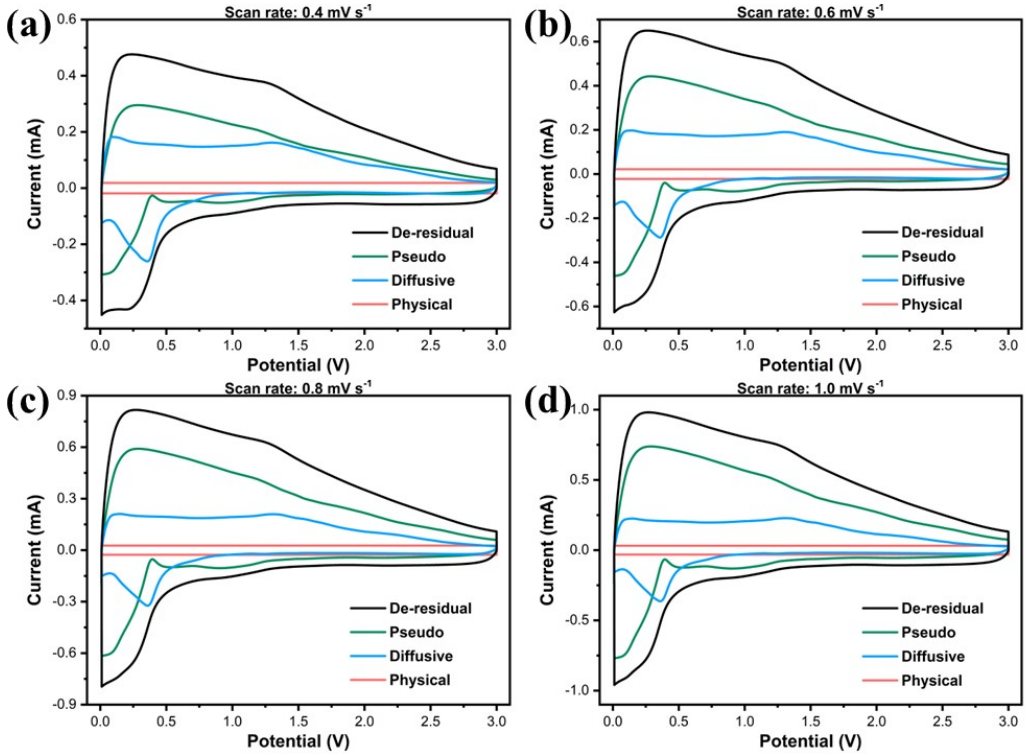

Figure S11 Details of pseudo, diffusion, and double-layer current in calibrated CV curves at 0.4-1.0 mV/s.

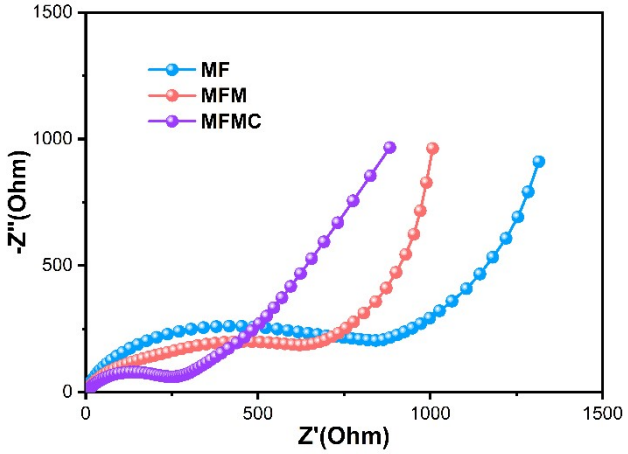

Figure S12 EIS curves of MF, MFM and MFMC.

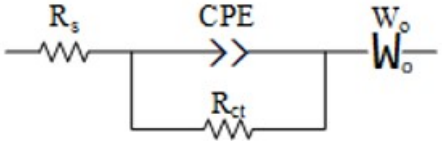

Figure S13 Equivalent circuit diagram of EIS.

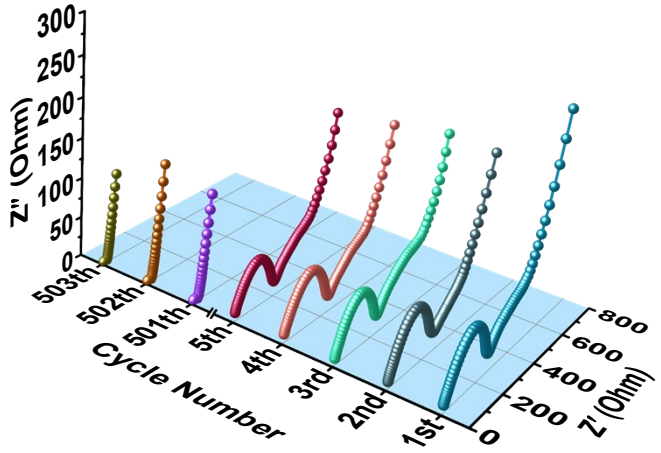

Figure S14 EIS curves of MFMC batteries in the charge state in different cycles.

Table S1 Comparison with other LiB researches about MnF_2 Anode

Electrode	Performance (1C = 577 mA g^{-1})	Ref.
MFMC	**1000 mA g^{-1}, 1300 cycles, 629 mAh g^{-1}**	**This work**
Octahedral MnF_2	100 mA g^{-1}, 200 cycles, 624.8 mAh g^{-1}	1
Hierarchical MnF_2	57.7 mA g^{-1}, 30 cycles, 986 mAh g^{-1}	2
Nano MnF_2	577 mA g^{-1}, 250 cycles, 359.2 mAh g^{-1}	3
MnF_2@NC	1000 mA g^{-1}, 700 cycles, 872.2 mAh g^{-1}	4
MnF_2/GNS	600 mA g^{-1}, 100 cycles, 489 mAh g^{-1}	5
Tetragonal MnF_2	100 mA g^{-1}, 1050 cycles, 330 mAh g^{-1}	6
CNT-MnF_2	57.7 mA g^{-1}, 100 cycles, 388 mAh g^{-1}	7
Ov-ZMF@NOFs	3000 mA g^{-1}, 400 cycles, 1012.6 mAh g^{-1}	8

Table S2 Varied Fitted impedances of discharged MFMC with cycling.

Cycle Number	$R_{ct}(\Omega)$
1st	279.4
2nd	228.4
3rd	227.8
4th	137.5
5th	126.7
501th	28.4
502th	31.1
503th	16.2

Table S3 Varied Fitted impedances of charged MFMC with cycling.

Cycle Number	$R_{ct}(\Omega)$
1st	229.8
2nd	250.3
3rd	201.5
4th	252.6
5th	234
501th	20.8
502th	16.2
503th	13.6

References

1 A. Jiao, Y. Duan, Z. Li, S. Zhang, T. Su and Z. Fu, *Electrochim. Acta*, 2024, **475**, 143595.

2 J. Lee, J. Im, J. R. Lee, H. Jang, J. Park, J. Lim, B. K. Cho and T. Kim, *J. Phys. Chem. Solids*, 2022,

161, 110477.
3 Y. Wei, X. Ma, C. Yang, B. Zhao, X. Zhu, C. Liang, Z. Zi and J. Dai, *J. Electroanal. Chem.*, 2019, **840**, 237-241.
4 S. Fang, J. Pei, L. Guo and Y. Qin, *Appl. Surf. Sci.*, 2024, **652**, 159323.
5 K. Rui, Z. Wen, Y. Lu, C. Shen and J. Jin, *Acs Appl. Mater. Interfaces*, 2016, **8**, 1819-1826.
6 A. Jiao, J. Gao, Z. He, J. Hou and L. Kong, *J. Energy Storage*, 2022, **47**, 103594.
7 N. Bensalah, D. Turki and K. Saoud, *Mater. Des.*, 2018, **147**, 167-174.
8 X. Tan, J. Liu, J. Huang, Y. Li, A. Zeb and X. Lin, *Energy Environ. Mater.*, 2023, **6**, e12436.